RESEARCH PAPER   OPEN ACCESS

Synthesis and characterization of chitosan-fruit peel nanocomposite with photocatalytic degradation from Tirupur industry dyes

P. Bhuvaneswari[1], S. Amutha[2], S. Vignesh[2], M. Sivakavinesan[2], T. Shanmugavadivu[1], G. Annadurai[2], E. Pushpalakshmi[2], S. Rajaduraipandian[1], E. Sindhuja*[1]

[1]*Department of Chemistry, Sri Paramakalyani College,*
Manonmaniam Sundaranar University, Alwarkurichi, Tamil Nadu, India
[2]*Sri Paramakalyani Centre of Excellence in Environmental Sciences,*
Manonmaniam Sundaranar University, Alwarkurichi, Tamil Nadu, India

Abstract
The high surface area-to-volume ratio of chitosan-fruit-peel nanocomposite and other distinctive physical, chemical, and biological properties that arise due to its size effects have attracted significant attention in the field of environmental remediation. Wet chemical techniques are commonly used to create metallic nanoparticles; however, the chemicals used are typically dangerous and combustible. Because it doesn't involve the use of hazardous chemicals, the synthesis of nanoparticles using a range of fruit resources is regarded as green technology. Utilizing the powdered peels of *Garcina mangostana* (mangosteen), the chitosan-fruit peel nanocomposite was created. By employing Fourier spectroscopy (FTIR), X-ray diffractometer (XRD), Field Emission Scanning Electron Microscopy (FESEM), and Thermogravimetric Analysis (TG/DTA), researchers were able to characterize the synthesized chitosan-fruit peel nanocomposite. Chitosan-fruit peel nanocomposite is used to investigate the photocatalytic degradation of model dye and industrial effluent. The sequestration of dye from aqueous solutions using chitosan-fruit peel nanocomposite is the main emphasis of this work. The Chitosan-Fruit Peel Nanocomposite could therefore be a viable adsorbent material in environmental rehabilitation and remediation.

*****Corresponding Author:** E. Sindhuja ✉ sindhujaelangovan@gmail.com

Introduction

India is well known for its high-quality textile items and has established itself as the major source of all high-end textile products. From India, clothing is exported to practically the entire developed world. Textiles and apparel account for 30% of India's exports, making them one of the major exporters (Smefdp-Sidbi, 2009). The greatest provider of services in India is the textile industry, which contributes 3% of the GDP.

In Tamilnadu, they are concentrated in Tiruppur and Karur, Punjab's Ludhiana, and Gujarat's Surat (Ranganathan *et al.*, 2007). According to Harvey (2008), the textile industry uses a lot of water and generates a lot of wastewater. The demand for textile products grows together with the production of textile wastewater, making the textile sector the primary cause of serious pollution issues on a global scale (Marimuthu *et al.*, 2015). If not properly treated, these effluents pose a serious hazard to human health and the environment since they contain a variety of chemicals and dyes, some of which are non-biodegradable and carcinogenic (Khehra *et al.*, 2006). The site becomes unusable for further construction as a number of harmful chemicals accumulate there.

The effluent-containing dyes are a significant cause of water contamination. According to Kumar *et al.* (2007), the wastewater produced by various textile mill production processes has high pH, temperature, detergents, oil, suspended and dissolved solids, leveling agents, hazardous and non-biodegradable matter, color, and alkalinity. The primary refractory organics, pigments, toxicants, and surfactants in textile wastewater are chlorinated compounds (AOX). According to Talarposhti *et al.* (2001), the chemical oxygen demand (COD), biochemical oxygen demand (BOD), pH, and color of textile wastewater are just a few of the many factors that fluctuate. According to (Alexander *et al.*, 2016), the purple mangosteen (*Garcinia mangostana*), also known simply as mangosteen, is a tropical evergreen tree that is thought to have its origins in the Indonesian islands of Sunda and the Moluccas.

Surface water and groundwater are combined to determine the textile industry's water requirements in Tiruppur. Groundwater is used by the plants in Tiruppur alone on an annual basis to the tune of 28.8 billion liters. Water is transported in transporters from nearby towns like Avinashi, Rayapuram, Murugampaliyam, and some locations in the neighboring Erode district. It is unnecessary to mention that Tiruppur has a simple water scarcity. Approximately 80% of the overall water demand is met by transporters. According to Sami *et al.* (2017), the textile units purchase water at a cost of Rs. 250–450 per transporter (12,000 liters capacity).

In this study, textile dye factories were taken out of an industrial aqueous solution using chitosan-fruit peel (mangosteen), which was used as a low-cost adsorbent. Investigated is how pH, dosages, and dye concentration affects degradation effectiveness. Through degradation tests, the reusability of the chitosan-fruit peel nanocomposite is evaluated. We were able to forecast the number of active sites engaged in the degradation of the pollutants to a thorough physicochemical analysis of our system and the management of the synthesis parameters, which were then compared with experimental adsorption data.

Materials and methods

Chitosan, which was obtained from crab shells bought at the Tirunelveli Fish Market, was combined with the following analytical-grade chemicals: hydrochloric acid, sodium hydroxide, ceric ammonium nitrate, methyl methacrylate, acrylic acid, sodium thiosulfate, manganese sulfate, sodium iodide, starch, potassium bromide, and nutrient agar. Wastewater from nearby textile dye factories was also used for the analysis.

Sample collection and water quality analysis

Water samples were taken in Tirupur, Tamil Nadu at three different places. Rayapuram industrial effluent water, Anaipalayam industrial effluent water, and the Noyyal river basin were collected the samples. Before noon, all water samples are collected and kept in clean BOD bottles and 5-liter bottles for water quality analysis. Corazol T blue (0.1g) was dissolved in

double-distilled water (100ml) and diluted to different concentrations (0.01g, 0.02g, and 0.03g) to create the solution.

Preparation of Chitosan
Waste spanner crab shells from regional restaurant suppliers were gathered in Tirunelveli. The shells were cleaned in deionized water and let to dry in the sun for 24 hours. The dried shells were broken down to 50-mesh particle size. Direct usage of 50-mesh crab shells was made for bio-sorption tests. Through a variety of chemical processes, including demineralization, deproteinization, deacetylation and decolorization, chitosan was removed from crab shells. The ground shells were demineralized by refluxing 5% HCl w/w over a period of 6 hours at room temperature.

The resulting solid was vacuum filtered after being dried and rinsed with deionized water until the pH was neutral. The resulting solid was deproteinized using a 5% NaOH solution, and the mixture was agitated at 80°C for 6 hours with a solid/solvent ratio of 1:10 (w/v). The residue was once more cleaned, filtered, and allowed to dry for 48 hours at room temperature. Deacetylation was carried out at 120°C for 24 hours using a solid/solvent ratio of 1:10 (w/v) and 45% NaOH. The resultant chitosan underwent a 6-hour process of sun drying to remove color. The chitosan nanoparticles were made using the obtained chitosan. The creation of chitosan from crab shells was investigated (Cadogan *et al.*, 2014a).

Preparation of chitosan nanocomposite
2g of chitosan were dissolved in 98ml of a 1% acetic acid solution to create a 2% chitosan solution. Chitosan nanoparticles were created using the inotropic gelation method (Shu and Zhu, 2001). After stirring through the N$_2$ gas for 20 minutes at room temperature, 2 g of dry fruit peel powder, 0.1 g of ceric ammonium nitrate, 1ml of methyl methacrylate, 1ml of acrylic acid, and starch were added to the chitosan solution. The N$_2$-treated chitosan nanocomposite solution was heated to 80°C in a water bath for 24 hours before being air dried. Then used grained to obtain the particles. These dried chitosan fruit peel nanocomposites were utilized for dye adsorption experiments after being cleaned with deionized water. The creation of a nanocomposite was depicted in studies (Cadogan *et al.*, 2014b).

Photocatalytic degradation of dyestuff
The effect of the different adsorbent dosages was (0.5 to 1.5 g L^{-1}) on the dye concentration (0.3g/L). Effect of varied pH values (4, 7.5, and 9) at constant on the dye concentration (0.3g/L) and adsorbent concentrations (0.1 g L^{-1}) were studied.

Using an Elico pH meter, the pH was adjusted by adding 0.1 M HCL and NaOH. A control setup was also kept going without any adsorbent addition. The suspensions were kept at room temperature in photocatalytic equipment before being exposed to radiation. Aliquots of 3ml solutions were filtered and utilized to assess the photocatalytic degradation of dye at the predetermined time interval.

Following this, the absorbance spectrum of the supernatant was determined using UV-Vis spectra at 381nm for model dye and industrial dye adsorption, 382nm (Noyyal river sample and Rayapuram industry effluent water, and 476nm (Anaipalayam industry effluent water.

Result and discussion
Fourier transforms infrared spectroscopy (FT-IR) analysis
The presence of a potential functional group for the production of chitosan nanoparticles is determined via FTIR analysis. Chitosan nanoparticles produced using green manufacturing techniques are reduced and stabilized as a result of these functional groups (Fig. 1). The prominent and broad peak in the 3500–3300 range in the chitosan spectra is attributable to hydrogen-bonded O–H stretching vibration.

According to Yu *et al.* (1999), the maxima for alkenes (-C=C- stretching) is 1680cm^{-1}, nitro compounds (N-O asymmetric stretching) are 1520cm^{-1}, and C-O stretching is 1090cm^{-1} and 809cm^{-1}, respectively.
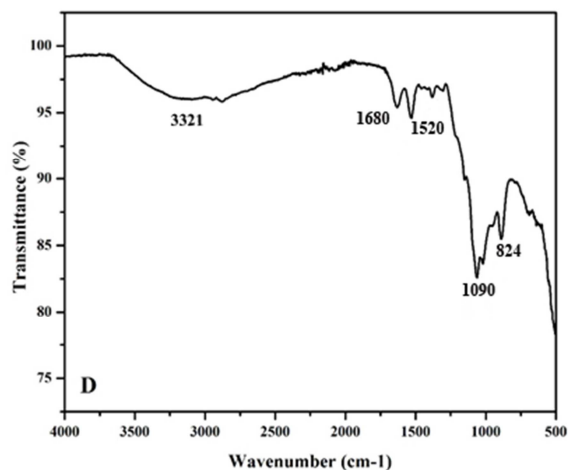
Fig. 1. FTIR spectra of synthesized chitosan nanoparticle.

To find the presence of a potential functional group for the synthesis of chitosan nanoparticles, FTIR analysis is performed. The stabilization and reduction of chitosan nanoparticles produced by green manufacturing are caused by these functional groups (Fig. 2). The hydrogen-bonded O-H stretching vibration is responsible for the prominent and broad peak in the 3500–3300 range in the chitosan spectra. Peaks for alkenes (-C=C stretching) are 1680cm⁻¹, nitro compounds (N-O asymmetric stretching) are 1520cm⁻¹, and C-O stretching is 1090cm⁻¹ and 809cm⁻¹, respectively (Yu *et al.*, 1999).
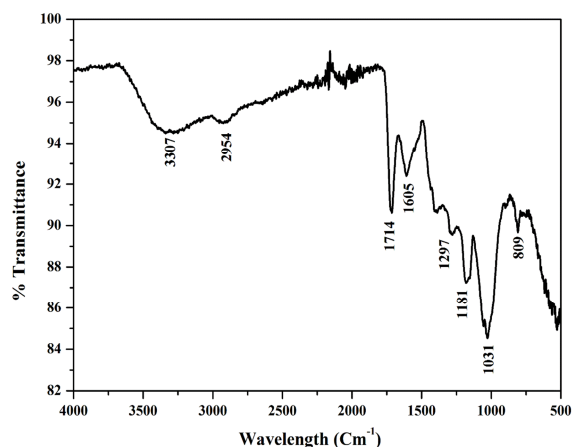
Fig. 2. FTIR spectra of chitosan-fruit peel nanocomposite.

Peaks of 1680cm⁻¹ and 1520cm⁻¹ shifted to 1764cm⁻¹ and 1605cm⁻¹, 1297cm⁻¹ and 1181cm⁻¹ peaks originating from nanocomposite; these shifting are due to plant extract being encapsulated in chitosan nanoparticles (Vijaya *et al.*, 2008).

Thermo Gravimetric Analysis (TGA)
TGA analysis is typically used to assess sample stability and weight loss throughout a range of temperatures. The TGA analysis of the chitosan-fruit nanocomposite in the current investigation revealed degradation patterns in four stages (Fig. 3). The release of water molecules caused a weight loss of 1.82mg in the first stage, which had a total mass of 13.51mg. Chitosan breakdown caused a weight loss (6.07mg) in the second stage, which was seen at 320.3°C. Decomposition-related weight loss (9.48mg) was seen in the third stage at 508° C. However, the two stages of weight loss caused by the chitosan's disintegration between 320 and 508 degrees Celsius were also investigated. Mostafa *et al.* (2012) Chitosan nanoparticle decomposition by TG analysis was published by (Parida *et al.*, 2013), and the report mentions two stages of decomposition at 365°C and 500°C.
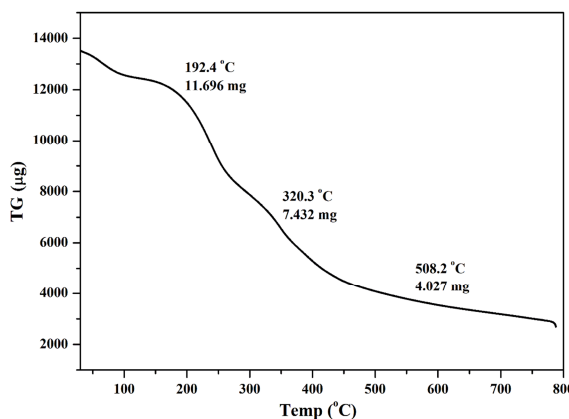
Fig. 3. Thermal degradation chitosan fruit peel nanocomposite.

X-Ray Diffraction analysis (XRD)
Both chitosan and chitosan fruit peel nanocomposite have been investigated in the 2 range of 10 -60 in the XRD examination. In the diffractogram of chitosan 2 values at 18.55°, 20.95°, 26.07°, and 31.88°, there is one strong peak, which is linked to the allomorphic tendency on the form of chitosan. The peaks are sharper, indicating the presence of crystal structure, as seen in Fig. 4. The ability for metal sorption may be constrained by the chitosan polymer's crystallinity.

The crystallinity sizes of the chitosan nanoparticles are 2 values of 38.68, 13.52, 17.02, and 39.22nm.
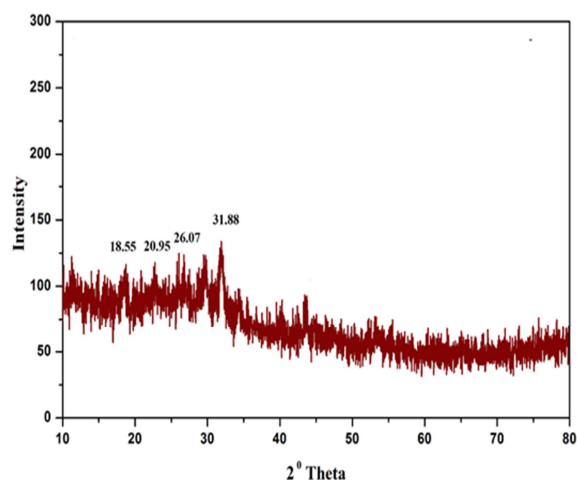
Fig. 4. XRD patterns of chitosan nanoparticle.
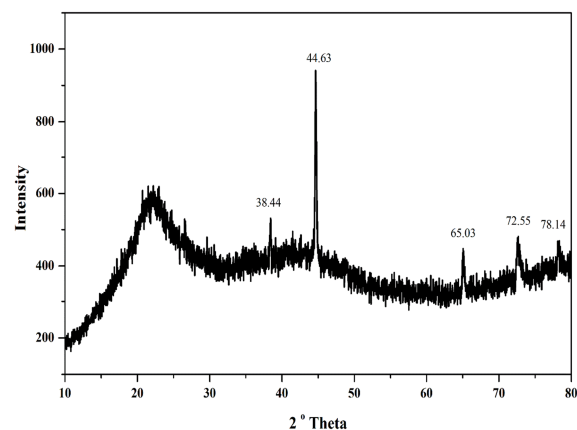
Fig. 5. XRD patterns of chitosan fruit peel nanocomposite.

The XRD pattern of the chitosan fruit peel nanocomposite is depicted in Fig. 5; multiple intensity peaks are seen at 2 values of 38.44°, 44.63°, 65.03°, 72.55°, and 78.14°, which correspond to crystallinity sizes of 66.56nm, 117.74nm, 34.25nm, 18.59nm, and 21. The crystallinity of the chitosan fruit peel nanocomposite (117.74nm) increases with the degree of deacetylation and is attributed to an expansion in intermolecular hydrogen bonding due to the presence of more free NH_2 groups (Higher Degree of Deacetylation) within the molecular structure, which leads to improved packing of the macromolecular polymeric chains and an increase in crystallinity (Parida *et al.*, 2013).

Field Emission Scanning Electron Microscope
On a nanoscale bar, the surface morphology of the chitosan fruit peel nanocomposite and nanoparticles was identified using a field emission scanning electron microscope (FESEM). The Chitosan nanoparticle's form and dispersion were seen in the FESEM image in Fig. 6
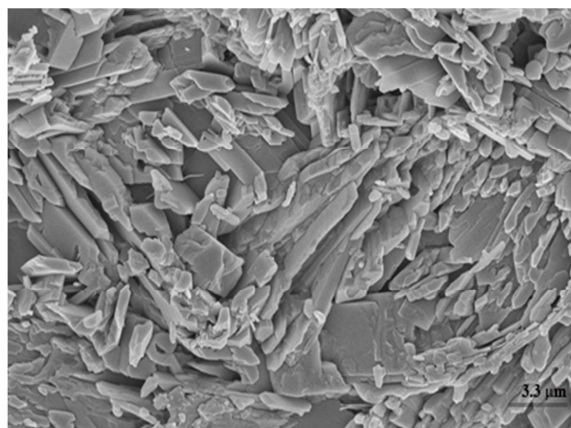
Fig. 6. FESEM image of poly-dispersed shaped chitosan nanoparticle.

The size of the chitosan nanoparticles ranges from 75 to 130nm, demonstrating that the particles are mainly poly-dispersed in shape and some combine into bigger particles with no clearly defined morphology. By employing macerated clove buds solution, researchers have observed similar irregular shapes of chitosan nanoparticles with diameters ranging from 5 to 100nm (Vanaja *et al.*, 2014; Sivakavinesan *et al.*, 2014). Chitosan fruit peel nanocomposite (Fig. 7) was found to have a poly-dispersed structure, with sizes ranging from 90 to 125nm.
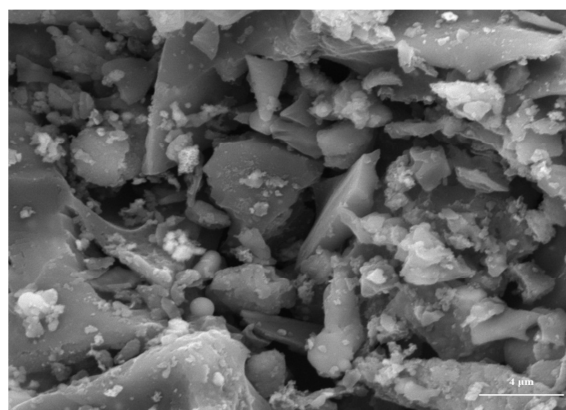
Fig. 7. FESEM image of poly-dispersed shaped chitosan fruit peel nanocomposite.

Photocatalytic degradation

According to calculations, the chitosan fruit peel nanocomposite's degradation efficiency was 36.3%, 34.9%, and 36.9% at 270 minutes for various adsorbent concentrations, as shown in Fig. 8-9 shows the percentages of 57.4, 42.4, and 32.1% at 270 minutes for different dye dosages, while Fig. 10 shows the percentages of 43.4%, 31.4%, and 38.1% at 270 minutes for various dye degradation pHs. Adsorption peak at 381nm in the visible range that changed during the reaction before disappearing altogether, indicating dye degradation (Slokar and Le Marechal 1998; Tanaka *et al.*, 2000).
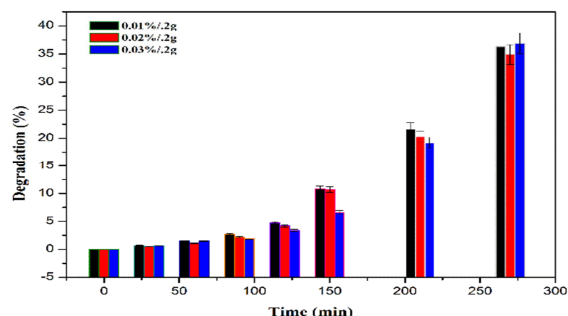
Fig. 8. Bar graph shows the degradation percentage of dye at different concentration.
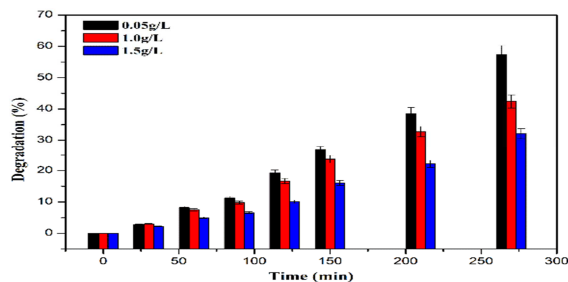
Fig. 9. Bar graph shows the degradation percentage of dye at different dosage.
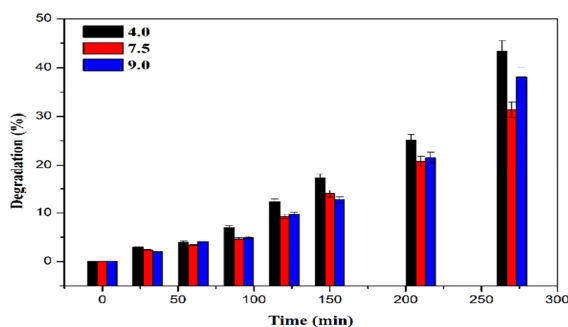
Fig. 10. Bar graph shows the degradation percentage of dye at different pH.

Photocatalytic reaction Experiments

The 1.5 L PyrexUV reactor used for the irradiation studies was wrapped in aluminum foil to improve reflection and fitted with a diving Philips HPK 125W high-pressure Tungsten lamp, which emits the most radiation at 365nm and also significantly at 435, 313, 253, and 404nm. In order to mimic the wavelengths of solar light reaching the earth's surface, a water-cooled Pyrex filter blocking the transmission of wavelengths below 290nm was hooked onto the lamp. The temperature was kept at 30-35°C using the tap water cooling circuit. Before and during the illumination, the dye solutions of 250ml volume (50mg L^{-1}, unless otherwise stated) were magnetically mixed with the appropriate amount of Chitosan fruit peel nanocomposite. With the exception of the tests looking at the impact of the initial pH, the solutions' pH, which varied to varying degrees, was not altered. Air was removed from the solution using an air pump and a flask containing a NaOH solution as a stopper in order to study the effects of aeration (Soutsas *et al.*, 2010; Sami *et al.*, 2017). The reactor was filled with solutions containing the necessary amount of dye and Chitosan fruit peel nanocomposite, and the suspensions were agitated magnetically. The light was turned on to start the photocatalytic reaction after 30 min of premixing in the dark to get the maximal adsorption of the dye onto the semiconductor surface. Chitosan fruit peel nanocomposite particles were removed from samples of 10ml by filtering them using a 0.45m Milli pore syringe filter at regular intervals.

Effect of initial dye concentration

It has been studied how different initial dye concentrations, ranging from 0.01 to 0.03mg L^{-1} at natural pH and Chitosan fruit peel nanocomposite loading of 1 g L^{-1} for Chitosan fruit peel nanocomposite, affect photocatalytic decolorization. As can be seen in Fig. 11, it was discovered that as dye concentration increases, the rate constant drops up to a point where zero-order reaction kinetics take over. According to Firmino *et al.* (2010), increasing the dye concentration from 0.01 to 0.03mg L^1 reduces the decolorization rate constant for Chitosan fruit peel nanocomposite from 80 to 300 min^1 and from 2 to 18mg/g from 30 to 80 min^1 correspondingly.
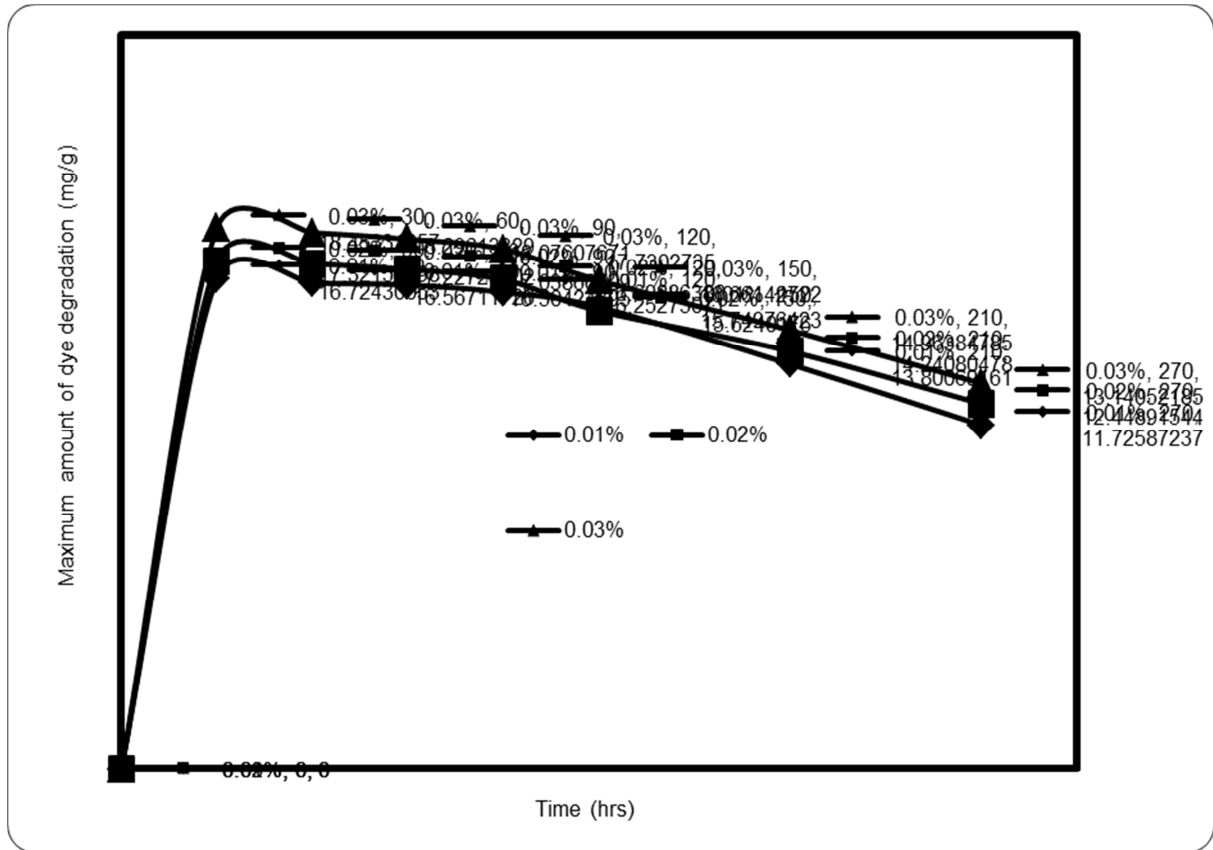
Fig. 11. Effect of Adsorbent Dosages.
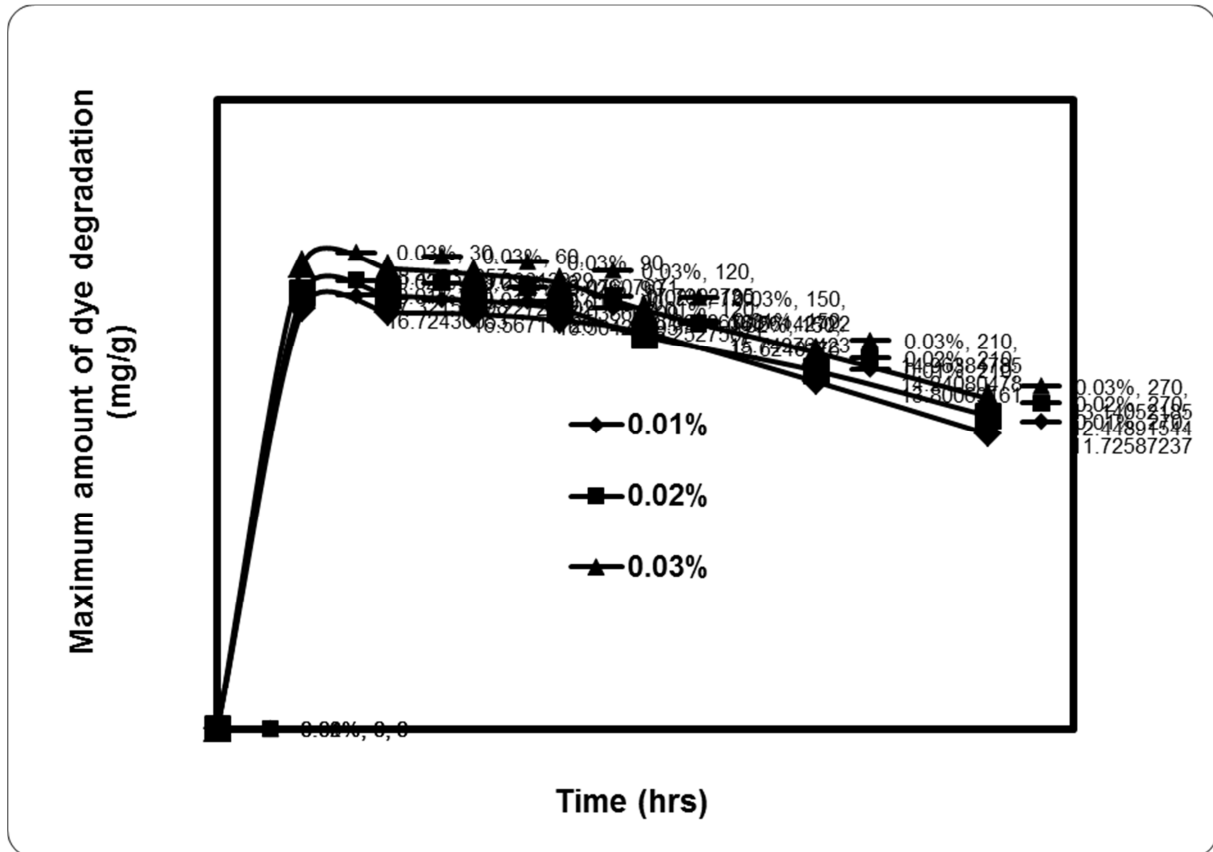
Fig. 12. Maximum amount of dye degradation of Model dye at different adsorbent dosages with time.

Using a photo reactor, the impact of chitosan fruit peel nanocomposite loading on the degradation of a model dye was examined while maintaining a constant value for all other parameters. As illustrated in Fig. 12, the apparent rate constant for the chitosan fruit peel nanocomposite at various concentrations is computed from the initial concentration and plotted against time. It is obvious that the constant rates rise with the concentration of chitosan fruit peel nanocomposite and peak at 0.05, 1.0, and 1.5 g/L L[1] chitosan fruit peel nanocomposite. The point at which the entire catalytic surface is fully lit varies on a number of variables, including the geometry and operating conditions of the reactor, the wavelength, and the intensity of the light source (Hameed and El-Khaiary, 2008a; Hameed et al., 2008b). The ideal catalyst loading is discovered to be reliant on the starting solute concentration because as the adsorbent dosage is increased; the total active surface area increases, making more active sites on the catalyst surface available. Particle aggregation may also lessen the adsorbent dosage activity at high concentrations by decreasing the specific surface,

Effect of solution pH

Solution pH is the primary factor that affects photocatalytic degradation. Using an initial concentration of 0.02mg L[1], a light intensity of 2.5 mWcm[2], and a chitosan fruit peel nanocomposite loading of 1 g L[1] for adsorbent doses, the effect of pH on the photocatalytic degradation of Model dye was investigated. In alkaline solutions, the pH was modified using NaOH, whereas in acidic solutions, it was altered using H_2SO_4 (Namasivayam and Kadirvelu, 1994; Namasivayam, 1995). Fig. 13 illustrates how changing the starting pH of an aqueous solution between 4.0 and 9.0 affects the apparent rate constant of photocatalytic degradation. Near the TiO_2 point of zero charges (pHpzc = 7.5), photocatalytic activity peaked, while the apparent rate constant decreased in alkaline circumstances. The results showed that the degradation apparent rate constant for chitosan fruit peel nanocomposite reduced with an increase in pH from 7.5 to 9.0, increased until the optimum (pH7.5), and

subsequently declined in an alkaline medium. The model color of degradation for chitosan fruit peel nanocomposite rises with an increase in pH from 7.5 to 9.0 (natural pH), and then falls in alkaline medium. It is clear from Fig.13 that the initial pH has a significant impact on the adsorption state, which is necessary to achieve maximum dye removal.

The association between dark adsorption and photocatalytic degradation was not seen in natural media, though. The molecular form of Model dye is typical at pH values less than 4.0, and the ionic form is typical at pH values higher than 7.5. The structure of the Model dye is in line with pH values. Both kinds of Model dye can be found at pH levels between 4.0 and 7.5. Since the chitosan fruit peel nanocomposite has a pH of around 7.5, its surface is positively charged in an acidic environment (pH 7.5) and negatively charged in an alkaline environment. The coupling of Model dye molecules with chitosan fruit peel nanocomposite particles is favored in acidic to neutral media due to the effect of charges attraction between negatively charged Model dye molecules and positively charged chitosan fruit peel nanocomposite particles.
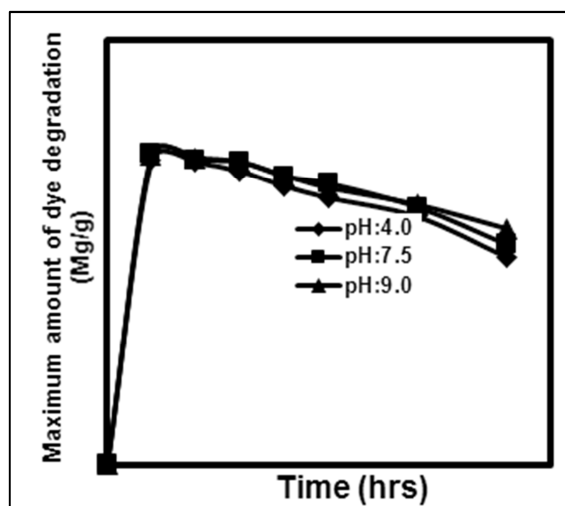
Fig. 13. Maximum amount of dye degradation of Model dye at different pH with time.

Due to the creation of an H-bond between the proton from the catalyst and the lone pair of electrons on the SO_3 group of the dye, the dye is firmly adsorbed on the photocatalyst in acidic solutions, which causes a significant degree of decolorization (Ong et al., 2010;

Ozdes *et al.*, 2010). Repulsive forces between negatively charged Model dye molecules (SO_3^- ions) and negatively charged chitosan fruit peel nanocomposite particles reduced the dye's adsorption at alkaline pH, where •OH was anticipated to be the dominant species.

Wastewater treatment-Photo catalytic degradation
In the process of treating wastewater, the pollutant concentration is a crucial factor. Real textile effluent was used in the studies to test the efficiency of semiconductor photocatalytic treatment. The wastewater's maximum absorbance wavelength, max = 550nm, was used to measure the wastewater's decolorization. Before beginning the biological treatment, the textile effluent was obtained and used directly, undiluted (Mary-Helen *et al.*, 2012; Min *et al.*, 2012).

Table 1. Characteristic of physical and chemical parameters for Industry wastewater.

Site	Site-1 (Noyyal river)	Site-2 (Rayapuram)	Site-3 (Anaipalayam)
pH at 37 °C	10.1±0.1	11.1±0.1	14.5±0.1
TDSmg / l	530	623	299
TSSmg / l	93	95	118
BOD_{5mg}/l	320	280	240
CODmg / l	512	448	416
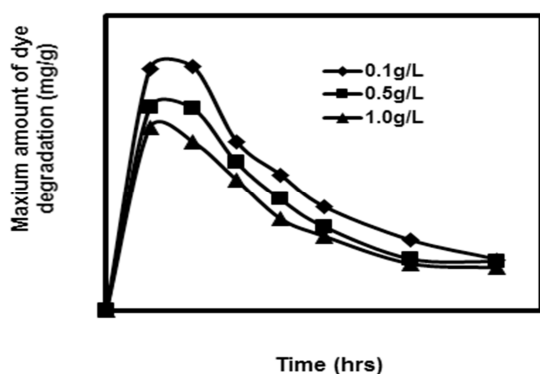
Fig. 14. Maximum amount of dye degradation of Industry wastewater at different Adsorbent dosages with time (NOYYAL River).

The sewage was examined. Table 1. Shows physical and chemical properties were investigated. The decolorization results for a 300-minute treatment are shown in Figs. 14, 15, and 16 for the dye concentration at Noyyal River, Rayapuram River, Anaipalayam

industry effluent water and Industry dye at the Site with constant composite concentration.
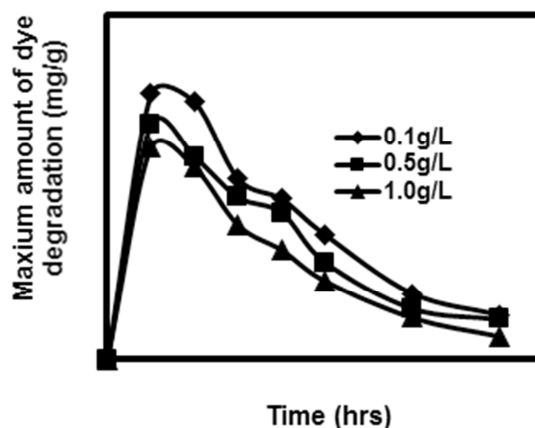
Fig. 15. Maximum amount of dye degradation of Industry wastewater at different Adsorbent dosages with time (RAYAPURAM - River).
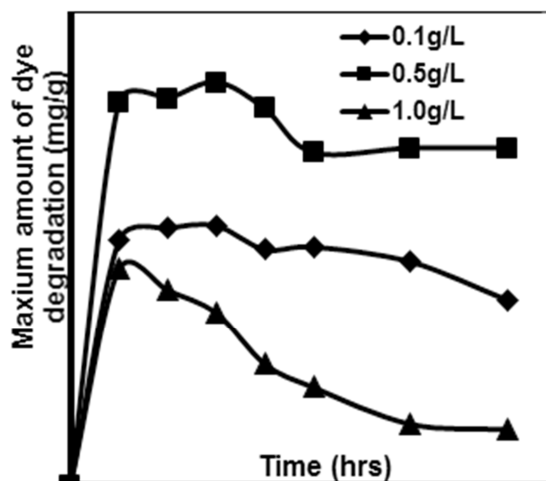
Fig. 16. Maximum amount of dye degradation of Industry wastewater at different Adsorbent dosages with time (ANAIPALAYAM - RIVER).

Complete decolorization of the wastewater was achieved within 300 min h, but the detoxification of the wastewater was only partly achieved (≈35% for 300 min treatment). It is obvious that prolonged irradiation is needed, in order to achieve total destruction of the contaminants, thus, resulting in the high cost of the method. However, when facing the problem of pollution the combination of methods could be the key to the total solution. Photocatalytic treatment in general has higher operating costs than those of a biological treatment.

However, it has been claimed that their usage as pre-treatment could improve the biodegradability of wastewater containing refractory pollutants, such as dyes. This would eliminate the need for total mineralization by allowing the intermediate reaction products to be destroyed by microorganisms in a biological post-treatment. From the standpoint of heterogeneous photocatalysis's practical applications, it is important to mention that this technique offers the chance to use solar radiation as well and can be chosen as one of the most well-liked solar technologies. Heterogeneous photocatalysis using chitosan fruit peel nanocomposite could be viewed as an alternative, promising method for the treatment of dye wastewater when this fact is combined with the efficiency of the procedure and the capability to be combined with other conventional technologies (Bizani *et al.*, 2006; Brintha *et al.*, 2012).

Conclusion

In the current study, *Garcinia mangostana* (mangosteen) is used to synthesize chitosan-fruit peel nanocomposites. The FTIR, XRD, TGA, and FESEM analyses are used to describe the synthesised nanocomposite. FTIR is used to determine the presence of functional groups, while TGA is used to evaluate the composite thermal degradation capacity. XRD examination reveals that the synthesised particles are crystalline. The synthesised nanocomposite is in poly dispersion shape, according to the FESEM investigation. For the photocatalytic degradation of Model and Industry dyes, a Chitosan-fruit peel nanocomposite has been created. With the help of photocatalysis and UV visible light, it is possible to effectively destroy the harmful chemical groups that Carozal T. blue and other dyes from the industry belong to. The photocatalytic oxidation depends on a number of variables, including pH, catalyst mass, oxidant addition, and the presence of naturally occurring chemicals. Before using the following components, it is important to precisely assess how they will affect dye degradation because their effects have occasionally been disputed and have appeared to depend on the type of substrate and on different experimental settings. Few researches

revealed full processes with precise reaction steps of the various pathways leading to multiple photoproducts; the majority of investigations on the photocatalytic degradation of Carozal T. blue and Industry dyes rely only on the monitoring of solution decolorization. Countless hours must be put towards quantifying these intermediates. Lack of quantitative information regarding the relative significance of the various degradation pathways will aid future mechanistic research on photocatalytic processes.

References

Alexander J, Jayanthi G, Lakshmipathy R, Kulasekaran A, Andal V. 2015. Colour removal studies on treatment of textile dyeing effluent by Chitosan modified Watermelon rind Composite (CWR). In National conference on Nanomaterials for Environmental [NCNER-2015] **8(5),** 10-15.

Bizani E, Fytianos K, Poulios I, Tsiridis V. 2006. Photocatalytic decolorization and degradation of dye solutions and wastewaters in the presence of titanium dioxide. Journal of Hazardous Materials **136(1),** 85-94.

Brintha SR, Sivakavinesan M, Soranam R, Annadurai G. 2012. Isotherm Studies on Adsorption of Crystal Violet Dye Using Zinc Oxide Adsorbents. International Journal of Chemical and Analytical Science **3(10),** 1573-1577

Cadogan EI, Lee CH, Popuri SR, Lin HY. 2014a. Effect of Solvent on Physico-Chemical Properties and Antibacterial Activity of Chitosan Membranes. International Journal of Polymeric Materials and Polymeric Biomaterials **63(14),** 708-715.

Cadogan EI, Lee CH, Popuri SR, Lin HY. 2014b. Efficiencies of chitosan nanoparticles and crab shell particles in europium uptake from aqueous solutions through biosorption: synthesis and characterization. International Biodeterioration & Biodegradation **95,** 232-240.

Firmino PIM, da Silva MER, Cervantes FJ, dos Santos AB. 2010. Colour removal of dyes from synthetic and real textile wastewaters in one-and two-stage anaerobic systems. Bioresource Technology **101(20),** 7773-7779.

Hameed BH, El-Khaiary MI. 2008a. Kinetics and equilibrium studies of malachite green adsorption on rice straw-derived char. Journal of Hazardous Materials **153(1),** 701-708.

Hameed BH, Mahmoud DK, Ahmad AL. 2008b. Sorption of basic dye from aqueous solution by pomelo (*Citrus grandis*) peels in a batch system. Colloids and Surfaces A: Physicochemical and Engineering Aspects **316(1),** 78-84.

Harvey FV. 2008. World water shortages growing 20 years ahead of predictions, Financial Times.

Khehra MS, Saini HS, Sharma DK, Chadha BS, Chimni SS. 2006. Biodegradation of azo dye CI Acid Red 88 by an anoxic-aerobic sequential bioreactor. Dyes and Pigments **1,** 1-7.

Kumar P, Prasad B, Mishra IM, Chand S. 2007. Catalytic thermal treatment of desizing wastewaters. Journal of Hazardous Materials **1,** 26-34.

Marimuthu KN, Ruby Thomas, Yamini B, Bharathi S, Murugavel K. 2015. Water Pollution due to Dying Effluents in Noyyal River, Tirupur- A Case Study. International Journal of ChemTech Research **7,** 3075-3080.

Mary-Helen S, Sivakavinesan M, Annadurai G. 2012. Equilibrium Studies on the Removal of Methyl Orange Dye from Aqueous Solution by Adsorption onto a Biopolymer. Drug Invention Today **4(11),** 590-593.

Min Y, Zhang K, Zhao W, Zheng F, Chen Y, Zhang Y. 2012. Enhanced chemical interaction between TiO_2 and graphene oxide for photocatalytic decolorization of methylene blue. Chemical Engineering Journal **193,** 203-210.

Mostafa Amin D, Adel Zak ES, Mohamed Mohamed AH, Dina Mohamed Diaa B. 2012. Thermal stability and degradation of chitosan modified by cinnamic acid. Open Journal of Polymer Chemistry **2(1),** 7.

Namasivayam C, Kadirvelu K. 1994. Coir pith, an agricultural waste by-product, for the treatment of dyeing wastewater. Bioresource Technology **48(1),** 79-81.

Namasivayam C. 1995. Adsorbents for the treatment of wastewater. In Trivedi RK, editor, Encyclopedia of environment production and control card, Maharashtra, India Vol. **1,** 30-49.

Ong SA, Uchiyama K, Inadama D, Ishida Y, Yamagiwa K. 2010. Treatment of azo dye Acid Orange 7 containing wastewater using up-flow constructed wetland with and without supplementary aeration. Bioresource Technology **101(23),** 9049-9057.

Ozdes D, Gundogdu A, Duran C, Senturk HB. 2010. Evaluation of adsorption characteristics of malachite green onto almond shell (*Prunus dulcis*). Separation Science and Technology **45(14),** 2076-2085.

Parida UK, Rout N, Bindhani BK. 2013. In vitro properties of chitosan nanoparticles induce apoptosis in human lymphoma SUDHL-4 cell line. Advances in Bioscience and Biotechnology **4(12),** 1118.

Ranganathan K, Karunagaran K, Sharma DC. 2007. Recycling of wastewaters of textile dyeing industries using advanced treatment technology and cost analysis—case studies. Resources, Conservation and Recycling **3,** 306-318.

Sami AJ, Khalid M, Iqbal S, Afzal M, Shakoori AR. 2017. Synthesis and Application of Chitosan-Starch Based Nanocomposite in Wastewater Treatment for the Removal of Anionic Commercial Dyes. Pakistan Journal of Zoology **49(1),** 21-26.

Shu XZ, Zhu KJ. 2001. Chitosan/gelatin microspheres prepared by modified emulsification and ionotropic gelation. Journal of Microencapsulation **18(2),** 237-245.

Sivakavinesan M, Malini M, Alagumuthu G, Annadurai G. 2014. Equilibrium and Response Surface Methodology Studies for Adsorption of Rhodamine B by Chitosan Nanoparticle. International Journal of Green and Herbal Chemistry **3(4),** 1408-1420.

Slokar YM, Le Marechal. 1998. Methods of decoloration of textile wastewaters. Dyes and Pigments **37(4),** 335-356.

Smefdp-Sidbi. 2009. Diagnostic study: Tiruppur Knitwear and Apparel Cluster, New Delhi, Apex Cluster Development Services.

Soutsas K, Karayannis V, Poulios I, Riga A, Ntampegliotis K, Spiliotis X, Papapolymerou G. 2010. Decolorization and degradation of reactive azo dyes via heterogeneous photocatalytic processes. Desalination **250(1),** 345-350.

Talarposhti AM, Donnelly T, Anderson GK. 2001. Color removal from simulated dye wastewater using a two-phase anaerobic packed bed reactor. Water Research **2,** 425-432.

Tanaka K, Padermpole K, Hisanaga T. 2000. Photocatalytic degradation of commercial azo dyes. Water Research **34(1),** 327-333.

Vanaja M, Paulkumar K, Baburaja M, Rajeshkumar S, Gnanajobitha G, Malarkodi C, Sivakavinesan M, Annadurai G. 2014. Degradation of methylene blue using biologically synthesized silver nanoparticles. Bioinorganic Chemistry and Applications **346,** 35-44

Vijaya Y, Popuri SR, Boddu VM, Krishnaiah A. 2008. Modified chitosan and calcium alginate biopolymer sorbents for removal of nickel (II) through adsorption. Carbohydrate Polymers **72(2),** 261-271.

Yu JH, Du YM, Zheng H. 1999. Blend films of chitosan-gelatin. Journal-Wuhan University Natural Sciences Edition **45,** pp.440-444.